

35. Singh, P. Degradation Physics of High Power LEDs in Outdoor Environment and the Role of Phosphor in the degradation process [Text] / P. Singh, C. M. Tan // Scientific Reports. – 2016. – Vol. 6. – P. 24052. doi: 10.1038/srep24052
36. Tan, C. M. Time Evolution Degradation Physics in High Power White LEDs Under High Temperature-Humidity Conditions [Text] / C. M. Tan, P. Singh // IEEE Transactions on Device and Materials Reliability. – 2014. – Vol. 14, Issue 2. – P. 742–750. doi: 10.1109/tdmr.2014.2318725
37. Amoabediny, G. H. Guidelines for safe handling, use and disposal of nanoparticles [Text] / G. H. Amoabediny, A. Naderi, J. Malakootikhah, M. K. Koochi, S. A. Mortazavi, M. Naderi, H. Rashedi // Journal of Physics: Conference Series. – 2009. – Vol. 170. – P. 012037. doi: 10.1088/1742-6596/170/1/012037

*В останні роки карстові ландшафти острова Кат Ба зазнали значного впливу внаслідок інтрузії та глобальних змін клімату. Природне руйнування карстових ландшафтів в результаті ерозії вапняку стає все більш розповсюдженою проблемою. Тому необхідно поглибити дослідження методів захисту для ефективного збереження ландшафтів*

*Ключові слова: Карстові ландшафти, Кат Ба, ерозія, ТМЕМ, вапняк*

*В последние годы карстовые ландшафты острова Кат Ба подверглись значительному воздействию вследствие интрузии и глобальных изменений климата. Естественное разрушение карстовых ландшафтов в результате эрозии известняка становится все более распространенной проблемой. Поэтому необходимо углубить исследования методов защиты для эффективного сохранения ландшафтов*

*Ключевые слова: Карстовые ландшафты, Кат Ба, эрозия, ТМЕМ, известняк*

UDC 550.8

DOI: 10.15587/1729-4061.2017.92168

## EROSION STUDY OF LIMESTONE ON THE Cat Ba ISLANDS IN NORTH EAST VIETNAM BY TRANSVERSE MICRO-EROSION METER

**Nguyen Trung Minh**

PhD, Associate Professor, Director\*

Email: nttminh@vast.vn

**Doan Dinh Hung**

Master of Science, Researcher\*

Email: doandinhhung@gmail.com

**Nguyen Thi Dung**

Master of Science, Researcher\*

Email: nguyendungVAST@gmail.com

**Tran Minh Duc**

Bachelor of Science, Researcher\*

Email: minhduc.hus@gmail.com

**Nguyen Ba Hung**

Bachelor of Science, Researcher\*

Email: hungdc53@gmail.com

**Cu Sy Thang**

Master of Science, Researcher

Institute of Geological Sciences

Vietnam Academy of Science and Technology

Alley 84 Chua Lang Street, Dong Da District, Hanoi, Vietnam

Email: cusythang@yahoo.com

\*Vietnam National Museum of Nature

Vietnam Academy of Science and Technology

Building A20, No.18 Hoang Quoc Viet Street,

Cau Giay Street, Hanoi, Vietnam

### 1. Introduction

The Cat Ba islands consisting of 367 islands are the third largest island group, behind The Phu Quoc and Cai Bau islands. However, The Cat Ba Islands are the biggest limestone islands in tropical Southeast Asia, also are the largest islands in Halong Bay Area with high potential for scientific

study. In recent years, tropical karst landscapes have been strongly affected by intrusion and impact of global climate changes. Therefore, understanding the processes of weathering, erosion and the effects of climatic factors and natural conditions on limestone weathering process is very essential, as a basis for proposing efficient conservation measures of sustainable natural heritage of our world (Fig. 1) [1].



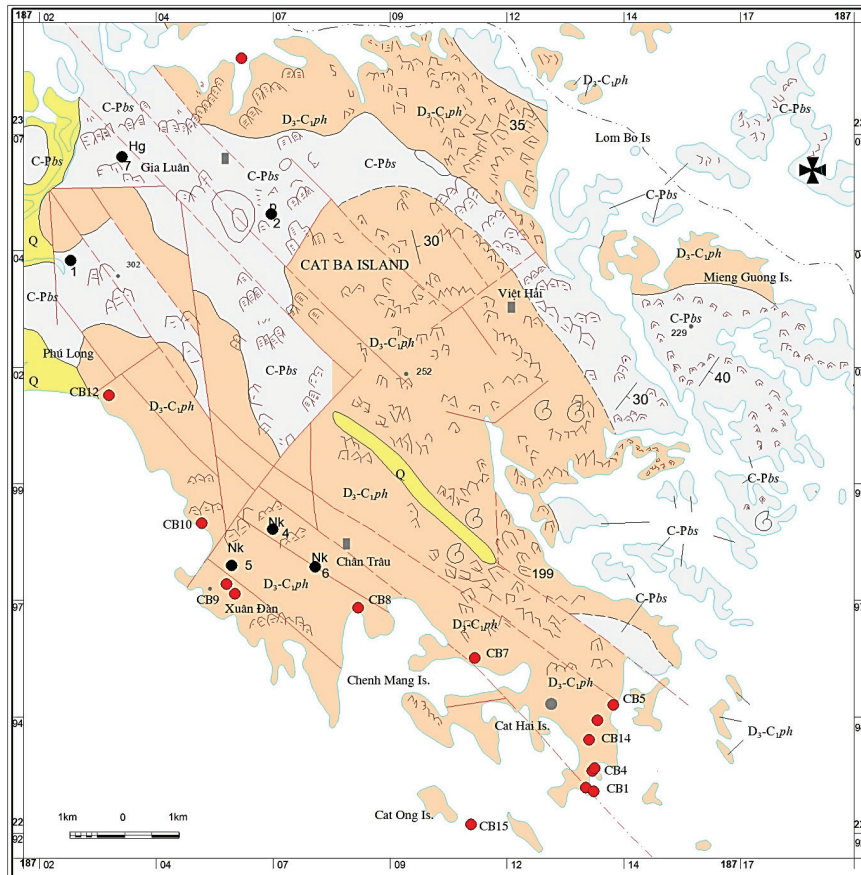
Fig. 1. Grey thick-bedded limestone, alternately with thick silicate of Pho Han Formation at CB1 exposure, near Cat Co 3 beach (N: 20°42'54,5"; E: 107°03'04,2")



Fig. 2. Massive White-grey Limestone of Bac Son Formation at CB12 exposure (N: 20°47'32,5"; E: 106°57'15,6")

Pho Han Formations (D3-C1ph) and Bac Son Formation (C-P bs) at

**CAT BA GEOLOGICAL MAP, HAI PHONG**



**LEGEND**

**I. STRATIGRAPHY**

- Q Quaternary: cohesionless pebble, granule, grit, sand, silt, mottled colour.
- C-Pbs Bac Son formation: Dark grey to light grey thick bedded or massive limestone, oolitic limestone, marl, cherty limestone.
- D<sub>3</sub>-C<sub>1</sub>ph Pho Han formation: Thick bedded limestone, grey zebra cherty limestone, chert, marl.

**II. OTHER SYMBOLS**

- Fault: a. Accurate b. Supposed
- Geological boundary: a. accurate b. supposed
- Strike and dip of beds
- Deposits and occurrences: 6- Number Hg: Mineral
- Fauna fossils
- Interesting geological place.
- Limestone mountains
- Survey points and numbers

Fig. 3. Geological map and sampling location map of Cat Ba Islands, Hai Phong

## 2. Literature review and problem statement

The micro-erosion meter (MEM) or traversing micro-erosion meter (TMEM) is the common method used to measure changes in the surface of the shore platform [5, 6]. The TMEM has since been used to measure small changes in surface elevation (usually downwearing) and weathering intensity on a variety of rock types in a wide range of environments. The method has undoubtedly improved our knowledge of the rates of erosion in the landscape, particularly how rates vary over short time and spatial scales. The method has also allowed more understanding of how different processes contribute to erosion in the landscape when careful experimental design is followed [7]. The relationships between these micro-scale changes and long-term changes in erosion rates can be quantified using this dataset. There are numerous studies reporting platform surface lowering, measured using the MEM or TMEM [1, 7]. These studies usually measured erosion over periods of about two years.

The application of TMEM methods in erosion study plays an important role in practical significance for the study of conservation research at the Cat Ba Islands. However, there is no study of MEM or TMEM on measuring the erosion rate in Vietnam, especially at the Cat Ba Islands. In this study, we provide 2 years TMEM results of limestone erosion at the Cat Ba Islands.

## 3. The aim and objectives of the research

Cat Ba islands consist mainly of limestone. In recent years, the karst landscape has been changed due to enhanced weathering (i. e., physical erosion and chemical dissolution) caused by global and local environmental change. Thus, understanding of erosion process at present and in future is highly needed to propose better preservation measures.

To achieve the aim, the following tasks are to be solved:

1. Several erosion stations will be constructed in a few representative islands selected based on topography, geology, and meteorological conditions.
2. Erosion stations were measured every two times each year.
3. In addition, rainfalls need to be measured.
4. Calculation erosion rate from the TMEM data.

## 4. Experimental conditions

The instrument consists of an engineer's gauge, mounted on a low, triangular frame, which measures the length of a probe extending to the rock surface below. When in use, the frame sits on three metal studs (a station) that are permanently embedded in the rock (Fig. 1, 2). The MEM allows repeated measurements, usually in 0.01 or 0.001 mm units, to be made of surface elevation and consequently of slow rock downwearing at three points. A later adaptation, the TMEM, permits numerous measurements to be made (100 or more, depending on instrument design and usage) within the triangular frame of the instrument. The precision and accuracy of the instrument are affected by variations in such factors as temperature and humidity, as well as by operator error [9].

Changes in elevation recorded at each point at a TMEM station are generally averaged to derive a mean rate of down-

wearing for that station. The probable difference between the mean derived from a limited number of sample points and the true population mean for the entire station surface depends upon the size of the sample and the degree of variation in the rate of downwearing within the station [10], Fig. 4.



Fig. 4. The calibration plate is used to set the gauge to zero

We have made 3 sets of locating pins for the TMEM. A recommendable procedure could be to first mark the positions with a compass, then drill a deep 5mm hole (which will keep the pin threaded rod vertical in place) and in the same hole position, drill a hole which has to be filled with an epoxy-based glue. The measurement of rock surface parameters was conducted on each sample by micro-erosion meter TMEM as a basis to calculate erosion rate, and to determine how the protrusions, rough or smooth rock surface is.

The calibration surface is a granite brick with a relatively flat surface (Fig. 4). Some pins are located on this surface as above. Calibrations should have been performed before each measurement. A calibration surface is also set up with locating pins for TMEM equipment. This surface is measured for calibration data before measuring a station. The relative erosion value at each point of each station is determined by the probable difference of measured value and calibration value at that point. It means that the calibration surface is set at erosion value "0" and used as a blank sample.

The measurement will be carried out in this calibration surface and field stations. Some given points in measured surface are recorded. For example, some results of one calibration measurement are in Table 1 below.

On calculating the relative erosion rate and modeling measurement, the data results were processed. In some gauge stations, surface parameters are not possible to be recorded (variable graph shows measured values with many horizontal sections at a value of 0) due to the distance between the probe and the surface of the sample is too large (maximum distance is 5 cm).

Relative erosion values of calibration surface

| Point of calibration surface | Relative Erosion Value 1 (mm) | Relative Erosion Value 2 (mm) | Relative Erosion Value 3 (mm) | Relative Erosion Value 4 (mm) | Mean Relative Erosion Value (mm) |
|------------------------------|-------------------------------|-------------------------------|-------------------------------|-------------------------------|----------------------------------|
| A1B4C1                       | 3.463                         | 3.488                         | 3.476                         | 3.458                         | 3.471                            |
| A2B5C1                       | 3.413                         | 3.348                         | 3.401                         | 3.396                         | 3.390                            |
| A3B6C1                       | 3.264                         | 3.269                         | 3.256                         | 3.258                         | 3.262                            |
| A4B7C1                       | 3.135                         | 3.137                         | 3.119                         | 3.143                         | 3.134                            |
| A5B8C1                       | 2.963                         | 2.915                         | 2.877                         | 2.951                         | 2.927                            |
| A6B9C1                       | 2.781                         | 2.743                         | 2.790                         | 2.799                         | 2.779                            |
| A7B10C1                      | 2.632                         | 2.640                         | 2.635                         | 2.631                         | 2.635                            |
| A8B11C1                      | 2.467                         | 2.475                         | 2.467                         | 2.483                         | 2.473                            |
| A9B12C1                      | 2.327                         | 2.323                         | 2.321                         | 2.326                         | 2.324                            |
| A10B13C1                     | 2.118                         | 2.161                         | 2.164                         | 2.180                         | 2.156                            |
| A1B5C2                       | 3.435                         | 3.463                         | 3.455                         | 3.463                         | 3.454                            |
| A2B6C2                       | 3.329                         | 3.332                         | 3.246                         | 3.320                         | 3.307                            |
| A3B7C2                       | 3.165                         | 3.025                         | 3.184                         | 3.165                         | 3.135                            |
| A4B8C2                       | 3.030                         | 3.020                         | 3.039                         | 3.024                         | 3.028                            |
| A5B9C2                       | 2.885                         | 2.879                         | 2.874                         | 2.877                         | 2.879                            |
| A6B10C2                      | 2.729                         | 2.720                         | 2.724                         | 2.748                         | 2.730                            |
| A7B11C2                      | 2.578                         | 2.578                         | 2.578                         | 2.583                         | 2.579                            |
| A8B12C2                      | 2.408                         | 2.415                         | 2.427                         | 2.433                         | 2.421                            |
| A9B13C2                      | 2.238                         | 2.277                         | 2.255                         | 2.281                         | 2.263                            |
| A1B6C3                       | 3.315                         | 3.322                         | 3.378                         | 3.321                         | 3.334                            |
| A2B7C3                       | 3.216                         | 3.240                         | 3.242                         | 3.243                         | 3.235                            |
| A3B8C3                       | 3.009                         | 3.079                         | 3.084                         | 3.055                         | 3.057                            |
| A4B9C3                       | 2.921                         | 2.905                         | 2.950                         | 2.957                         | 2.933                            |
| A5B10C3                      | 2.827                         | 2.825                         | 2.831                         | 2.828                         | 2.828                            |
| A6B11C3                      | 2.682                         | 2.698                         | 2.658                         | 2.688                         | 2.682                            |
| A7B12C3                      | 2.543                         | 2.538                         | 2.502                         | 2.536                         | 2.530                            |
| A8B13C3                      | 2.381                         | 2.378                         | 2.370                         | 2.369                         | 2.375                            |
| A1B7C4                       | 3.261                         | 3.202                         | 3.250                         | 3.231                         | 3.236                            |
| A2B8C4                       | 3.131                         | 3.118                         | 3.164                         | 3.133                         | 3.137                            |
| A3B9C4                       | 3.043                         | 3.044                         | 3.043                         | 3.040                         | 3.043                            |
| A4B10C4                      | 2.893                         | 2.898                         | 2.898                         | 2.895                         | 2.896                            |
| A5B11C4                      | 2.775                         | 2.775                         | 2.773                         | 2.778                         | 2.775                            |
| A6B12C4                      | 2.616                         | 2.623                         | 2.620                         | 2.617                         | 2.619                            |
| A7B13C4                      | 2.464                         | 2.461                         | 2.443                         | 2.461                         | 2.457                            |
| A1B8C5                       | 3.259                         | 3.259                         | 3.256                         | 3.242                         | 3.254                            |
| A2B9C5                       | 3.129                         | 3.157                         | 3.130                         | 3.138                         | 3.139                            |
| A3B10C5                      | 2.989                         | 2.978                         | 2.960                         | 2.984                         | 2.978                            |
| A4B11C5                      | 2.849                         | 2.858                         | 2.859                         | 2.852                         | 2.855                            |
| A5B12C5                      | 2.797                         | 2.744                         | 2.713                         | 2.706                         | 2.740                            |
| A6B13C5                      | 2.560                         | 2.588                         | 2.552                         | 2.553                         | 2.563                            |
| A1B9C6                       | 3.211                         | 3.213                         | 3.218                         | 3.117                         | 3.190                            |
| A2B10C6                      | 3.028                         | 3.086                         | 3.084                         | 3.061                         | 3.065                            |
| A3B11C6                      | 2.946                         | 2.945                         | 2.943                         | 2.934                         | 2.942                            |
| A4B12C6                      | 2.701                         | 2.785                         | 2.791                         | 2.777                         | 2.764                            |
| A5B13C6                      | 2.640                         | 2.651                         | 2.647                         | 2.652                         | 2.648                            |
| A1B10C7                      | 3.164                         | 3.167                         | 3.133                         | 3.124                         | 3.147                            |
| A2B11C7                      | 3.035                         | 3.034                         | 3.038                         | 3.033                         | 3.035                            |
| A3B12C7                      | 2.890                         | 2.892                         | 2.886                         | 2.890                         | 2.890                            |
| A4B13C7                      | 2.683                         | 2.667                         | 2.736                         | 2.738                         | 2.706                            |
| A1B11C8                      | 3.133                         | 3.136                         | 3.138                         | 3.133                         | 3.135                            |
| A2B12C8                      | 2.999                         | 2.984                         | 2.985                         | 2.973                         | 2.985                            |
| A3B13C8                      | 2.823                         | 2.835                         | 2.813                         | 2.843                         | 2.829                            |
| A1B12C9                      | 3.085                         | 3.087                         | 3.082                         | 3.081                         | 3.084                            |
| A2B13C9                      | 2.931                         | 2.929                         | 2.932                         | 2.926                         | 2.930                            |
| A1B13C10                     | 3.034                         | 3.040                         | 3.045                         | 3.032                         | 3.038                            |

The formula for calculating the relative erosion value and rate at each measurement point is as follows: Relative erosion value of A time = Measured relative erosion value of n time – Value of calibration surface of A time.

Relative erosion rate = (Relative erosion value at A time – Relative erosion value at B time) \* 365 / total counted days from A time to B time).

Unit of relative erosion rate in the formula is mm/year, Fig. 5.



Fig. 5. TMEM instrument is used to determine erosion rate at some stations on limestone sampled in Cat Ba islands

Surface parameters of rock stations located in the Cat Ba archipelago are initial results of the initial research of weathered limestone of eroded Cat Ba islands by impacts of rain, wind, sun [11]. Distributed areas of some stations in the study include shallow zone, intertidal and sub-tidal zone.

## 5. The results

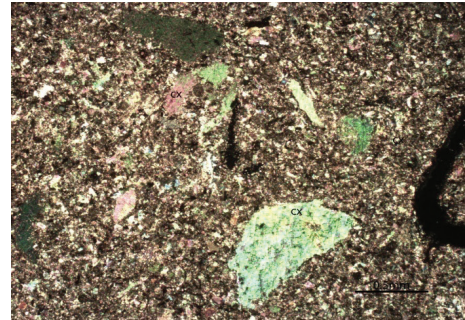
### 5. 1. Characteristics of petrographic compositions

The analytical results of petrography of 3 grey limestone sections of Pho Han Formation and Bac Son Formation are the following.

*Sample CB5*, thin-bedded limestone of Pho Han Formation, is determined as heterogeneous recrystallized calcilith (Fig. 6, a, b). Apparently, this sample is dark grey, fine grain with dubiocrystalline massive structure and strongly reacted with hydrochloric acid 5 %. It is phenoclastic texture, vector structure with mineral composition, including Calcite 95–97 %, Dolomite 3–5 %, less quartz, carbonaceous materials, and ore.

*Sample CB10*, dark grey massive limestone of Pho Han Formation, in thin section dolomite limestone is defined: dark grey, fine grain, dubiocrystalline, massive structure and strongly reacted with hydrochloric acid 5 % (Fig. 7, a, b). This section has opalescence vein, phenoclastic texture and vector structure.

*Sample CB12*, light grey limestone of Bac Son Formation, are defined as white grey, fine grain, dubiocrystalline dolomite with dubiocrystalline, massive structure and light reacted with acid chlorhidric 5 %. Mineral compositions include dolomite 95 %, calcite 5 %, less ores (Fig. 8, a, b).

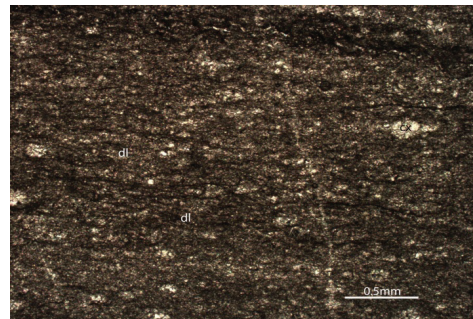


a

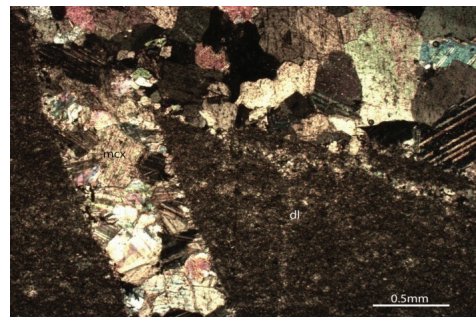


b

Fig. 6. Micropatcal calcite (cx), granulated calcite and recrystallizational calcite: a – heterogeneous recrystallizational (Nicol +); b – with clear face in heterogeneous recrystallizational limestone bedded metabasis (Nicol +)



a



b

Fig. 7. Automorphic-granular dolomite (dl): a – Micropartical dolomite (dl), carbonaceous affected- granulated dolomite in dolomite – calcylite rocks. Nicol (+); b – Rock background mainly consists of micropartical dolomite, granulated dolomite (dl) are interpenetrated by hydrothermal calcite vein. Nicol (+)

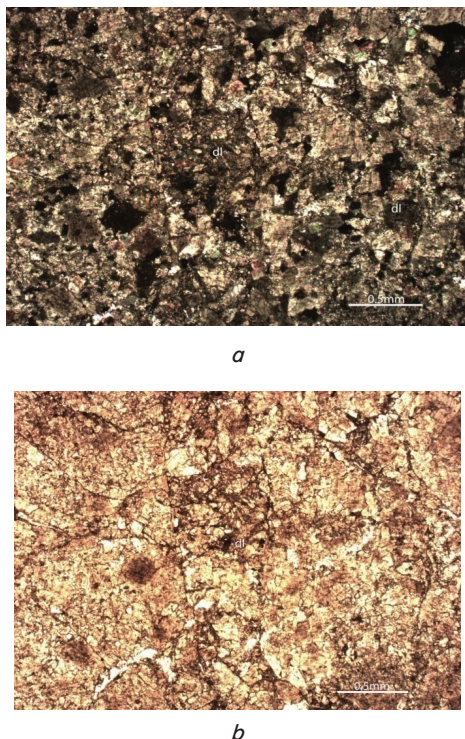


Fig. 8. Automorphic-granular dolomite (dl): *a* – with various particle sizes in dolomite rocks. Nicol (+); *b* – with aphanitic – fine – medium size in dolomite rocks. Nicol (-)

5. 2. Erosion

Results of limestone weathering and erosion in Cat Ba Islands on April 8th, 2015 and November 9th, 2015 are shown below (Fig. 9, Table 2).

Station X2, X6 – Grey-white limestone of BacSon Formation.

Station Y1, Y5 – Siliceous grey-black of PhoHan Formation.

Station Z5, Z7 –thin-bedded grey limestone of PhoHan Formation.

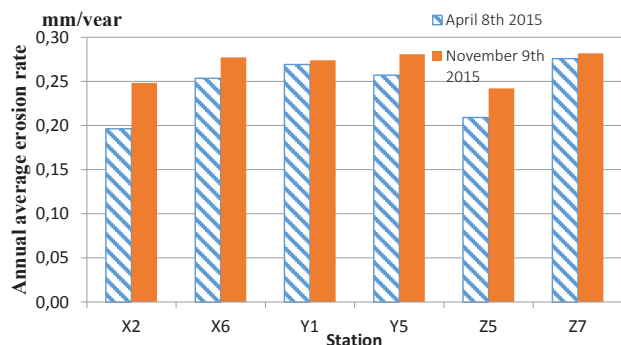


Fig. 9. Column graph of relative erosion rates recorded from some stations on limestone sampled in the Cat Ba Archipelago on April 8th, 2015 and November 9th, 2015

It can be noticed that results of the relative erosion rate on April 8th, 2015 are lower than on November 9th, 2015. Total rainfall values counted from the beginning of the study (July 1st, 2014) to the first measuring date (April 8th, 2015) and the second measuring date (November 9th, 2015)

are 980.2 mm and 2280 mm, respectively (Fig. 10). Total rainfall value in the period from the first time to the second time is 1299.8 mm. Therefore, the erosion rate of limestone is strongly affected by changes of total rainfall on the Cat Ba Island.

Table 2

Annual average erosion rate values recorded at 6 measured stations on April 8th, 2015 and November 9th, 2015

| Station | Annual average erosion rate (mm/year) |                    |
|---------|---------------------------------------|--------------------|
|         | April 8th, 2015                       | November 9th, 2015 |
| X2      | 0.1964                                | 0.2481             |
| X6      | 0.2537                                | 0.2773             |
| Y1      | 0.2691                                | 0.2738             |
| Y5      | 0.2573                                | 0.2808             |
| Z5      | 0.2092                                | 0.2420             |
| Z7      | 0.2759                                | 0.2818             |

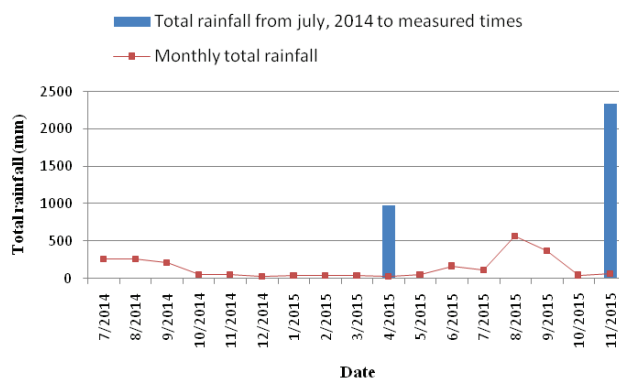


Fig. 10. Total rainfall data on Cat Ba islands (from July 2014 to November 2015)

The stations Y7, Y8 and Z1 are measured in recent dates, on April 2016. For station Y7, the lowest erosion value point recorded in Station Y7 is about 0.004 mm, respectively  $2.28 \times 10^{-3}$  mm/year, and the highest of 0.626 mm respectively 0.357 mm/year. Average erosion value is 0.24 mm, so the average rate of annual erosion in Station Y7 is 0.137 mm (Table 3, Fig. 11). Thereby, we can see a big impact on the speed of seawater corrosion of limestone.

In Table 4, the lowest erosion point A2B12C8 recorded in station Y8 is 0.081 mm corresponded with the erosion rate of 0.203 mm/year, compared with the highest value 0.321 mm at point A6B9C1 and erosion rate 0.803 mm/year correspondingly. Average erosion value is about 0.188 mm, so the annual average erosion rate at station Y8 is about 0.509 mm. This high-level erosion rate needs to be studied for a long time. Only station Z1 was located in the surf zone, not in full-time study. It has been relocated into the submerged zone after a first 10-month period of the study (from July 2014 to April 2015). In Table 5, the highest erosion value recorded in this station was 0.624 mm at measuring point A4B8C2, correspondingly erosion rate of 0.356 mm/year.

Table 3

Measured erosion rate values measured at Station Y7 (on July 2nd, 2014 and April 2nd, 2016)

| Point of Station Y7 | Measured value (July 2nd, 2014) |                      |                                 | Measured value (April 2nd, 2016) |                      |                                 | Erosion rate value (mm/year) |
|---------------------|---------------------------------|----------------------|---------------------------------|----------------------------------|----------------------|---------------------------------|------------------------------|
|                     | Average value (mm) (1)          | Calibration (mm) (2) | Relative average value (mm) (3) | Average value (mm) (4)           | Calibration (mm) (5) | Relative average value (mm) (6) |                              |
| A1B4C1              | 4.555                           | 3.733                | 8.287                           | 4.332                            | 3.753                | 8.085                           | 0.115                        |
| A2B5C1              | 4.495                           | 3.644                | 8.139                           | 4.173                            | 3.661                | 7.834                           | 0.174                        |
| A9B12C1             | 0.762                           | 2.754                | 3.516                           | 0.653                            | 2.740                | 3.392                           | 0.071                        |
| A10B13C1            | 0.134                           | 2.619                | 2.753                           | 0.015                            | 2.580                | 2.595                           | 0.090                        |
| A3B7C2              | 3.887                           | 3.487                | 7.373                           | 3.682                            | 3.419                | 7.102                           | 0.155                        |
| A8B12C2             | 1.255                           | 2.802                | 4.057                           | 1.178                            | 2.782                | 3.960                           | 0.056                        |
| A6B11C3             | 2.666                           | 3.073                | 5.738                           | 2.586                            | 3.032                | 5.617                           | 0.069                        |
| A2B8C4              | 5.066                           | 3.539                | 8.605                           | 4.930                            | 3.498                | 8.427                           | 0.102                        |
| A5B11C4             | 4.028                           | 3.160                | 7.188                           | 3.446                            | 3.116                | 6.562                           | 0.357                        |
| A6B12C4             | 3.451                           | 2.941                | 6.392                           | 3.015                            | 2.925                | 5.940                           | 0.258                        |
| A7B13C4             | 2.806                           | 2.881                | 5.687                           | 2.414                            | 2.818                | 5.232                           | 0.260                        |
| A2B9C5              | 4.934                           | 3.511                | 8.445                           | 4.944                            | 3.462                | 8.406                           | 0.022                        |
| A3B10C5             | 4.737                           | 3.378                | 8.115                           | 4.647                            | 3.327                | 7.973                           | 0.081                        |
| A5B12C5             | 3.206                           | 3.103                | 6.309                           | 3.168                            | 3.055                | 6.223                           | 0.049                        |
| A6B13C5             | 3.374                           | 2.985                | 6.359                           | 2.861                            | 2.920                | 5.781                           | 0.330                        |
| A2B10C6             | 5.152                           | 3.467                | 8.619                           | 4.874                            | 3.422                | 8.296                           | 0.184                        |
| A3B11C6             | 4.941                           | 3.333                | 8.274                           | 4.995                            | 3.275                | 8.269                           | 0.002                        |
| A2B12C8             | 4.789                           | 3.372                | 8.161                           | 4.675                            | 3.330                | 8.005                           | 0.089                        |

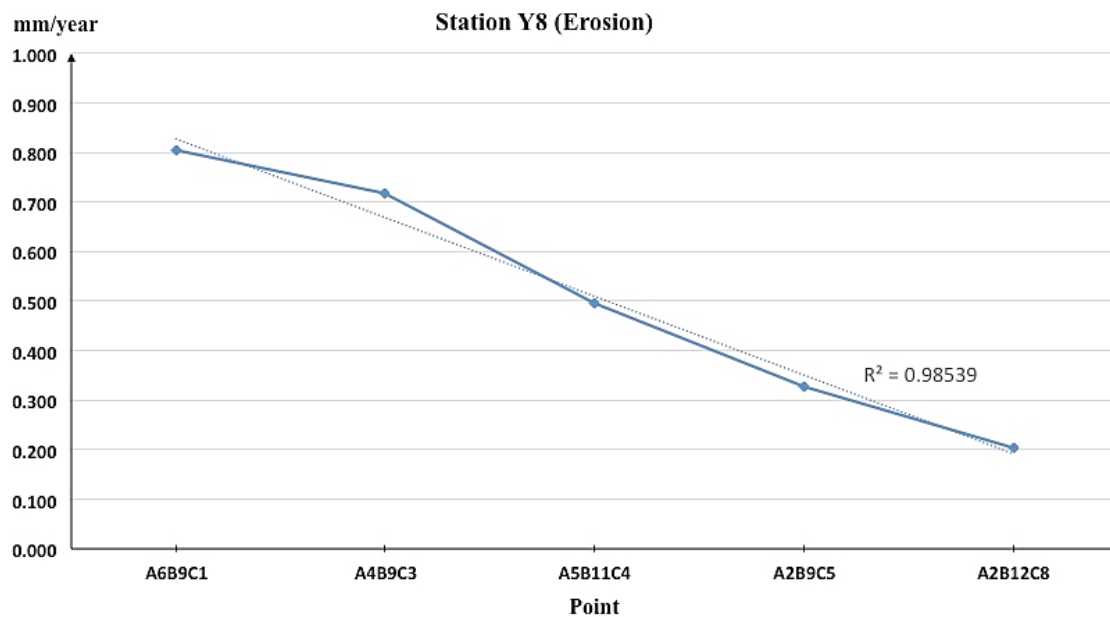


Fig. 11. Line graph of erosion trend recorded at station Y8

Table 4

Measured erosion rate values measured at Station Y8 (on November 9th, 2015 and April 2nd, 2016)

| Point of Station Y8 | Measured value (November 9th, 2015) |                      |                                 | Measured value (April 2nd, 2016) |                      |                                 | Erosion rate value (mm/year) |
|---------------------|-------------------------------------|----------------------|---------------------------------|----------------------------------|----------------------|---------------------------------|------------------------------|
|                     | Average value (mm) (1)              | Calibration (mm) (2) | Relative average value (mm) (3) | Average value (mm) (4)           | Calibration (mm) (5) | Relative average value (mm) (6) |                              |
| A6B9C1              | 6.360                               | 3.164                | 3.197                           | 6.030                            | 3.154                | 2.875                           | 0.803                        |
| A4B9C3              | 6.772                               | 3.273                | 3.499                           | 6.512                            | 3.300                | 3.212                           | 0.717                        |
| A5B11C4             | 6.451                               | 3.072                | 3.379                           | 6.296                            | 3.116                | 3.180                           | 0.497                        |
| A2B9C5              | 5.228                               | 3.414                | 1.814                           | 5.146                            | 3.462                | 1.683                           | 0.327                        |
| A2B12C8             | 6.259                               | 3.288                | 2.971                           | 6.220                            | 3.330                | 2.890                           | 0.203                        |

Table 5

Measured erosion rate values measured at Station Z1 (on July 2nd, 2014 and April 2nd, 2016)

| Point of Station Y8 | Measured value (July 2nd, 2014) |                      |                                 | Measured value (April 2nd, 2016) |                      |                                 | Erosion rate value (mm/year) |
|---------------------|---------------------------------|----------------------|---------------------------------|----------------------------------|----------------------|---------------------------------|------------------------------|
|                     | Average value (mm) (1)          | Calibration (mm) (2) | Relative average value (mm) (3) | Average value (mm) (4)           | Calibration (mm) (5) | Relative average value (mm) (6) |                              |
| A1B4C1              | 3.253                           | 3.733                | -0.480                          | 3.268                            | 3.753                | -0.485                          | 0.003                        |
| A2B5C1              | 3.527                           | 3.644                | -0.117                          | 3.528                            | 3.661                | -0.133                          | 0.009                        |
| A4B8C2              | 5.836                           | 3.373                | 2.463                           | 5.742                            | 3.358                | 2.384                           | 0.045                        |
| A4B9C3              | 5.481                           | 3.327                | 2.154                           | 4.830                            | 3.300                | 1.530                           | 0.356                        |

The lowest erosion value and erosion rate recorded at measuring point A1B4C1 are 0.005 mm and 0.003 mm/year, respectively. Recorded data is not enough for overall erosion assessment at this station.

**5. 3. Accretion**

It can be shown that strong accretion occurs on the surface station Z1 due to place in the surf zone (Fig. 12).

The largest value recorded is 0.722mm (point A5B10C3), compared with the lowest value of 0.034 mm in point A3B6C1. Therefore, the annual accretion rate at this station ranged from 0.019 to 0.412 mm, corresponding with 0.195 mm/year in average, in calculation. This is a high-level accretion trend with linear coefficient of determination  $R^2$  of 0.975. It should be monitored and investigated in a long time to get more accurate results (Table 6).

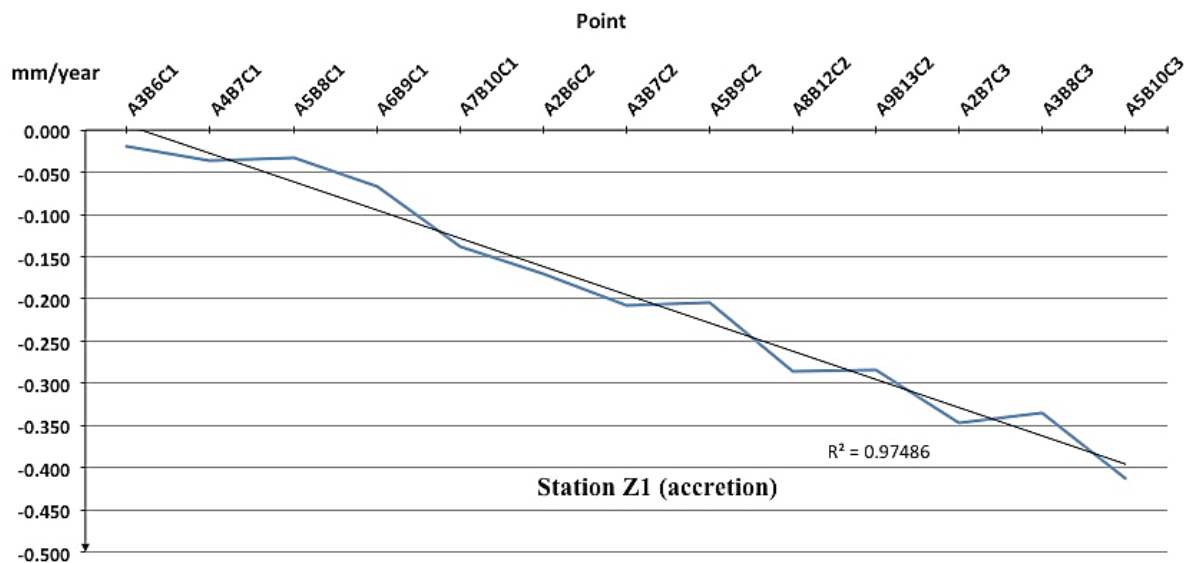


Fig. 12. Line graph of accretion trend recorded at station Z1

Table 6

Measured accretion values measured at Station Z1 (on July 1st, 2014 and April 2nd, 2016)

| Point of Station Z1 | Measured value (July 1st, 2014) |                      |                                 | Measured value (April 2nd, 2016) |                      |                                 | Accretion rate value (mm/year) |
|---------------------|---------------------------------|----------------------|---------------------------------|----------------------------------|----------------------|---------------------------------|--------------------------------|
|                     | Average value (mm) (1)          | Calibration (mm) (2) | Relative average value (mm) (3) | Average value (mm) (4)           | Calibration (mm) (5) | Relative average value (mm) (6) |                                |
| A3B6C1              | 3.729                           | 3.506                | 0.223                           | 3.783                            | 3.527                | 0.257                           | -0.019                         |
| A4B7C1              | 3.510                           | 3.388                | 0.122                           | 3.593                            | 3.408                | 0.185                           | -0.036                         |
| A5B8C1              | 6.055                           | 3.281                | 2.774                           | 6.116                            | 3.286                | 2.830                           | -0.032                         |
| A6B9C1              | 5.623                           | 3.145                | 2.478                           | 5.749                            | 3.154                | 2.595                           | -0.067                         |
| A7B10C1             | 5.352                           | 3.038                | 2.314                           | 5.581                            | 3.026                | 2.555                           | -0.138                         |
| A2B6C2              | 3.591                           | 3.607                | -0.015                          | 3.885                            | 3.602                | 0.283                           | -0.171                         |
| A3B7C2              | 3.494                           | 3.487                | 0.007                           | 3.789                            | 3.419                | 0.370                           | -0.207                         |
| A5B9C2              | 5.670                           | 3.237                | 2.433                           | 5.995                            | 3.204                | 2.791                           | -0.205                         |
| A8B12C2             | 5.029                           | 2.802                | 2.227                           | 5.509                            | 2.782                | 2.727                           | -0.286                         |
| A9B13C2             | 4.774                           | 2.657                | 2.117                           | 5.253                            | 2.640                | 2.613                           | -0.283                         |
| A2B7C3              | 3.325                           | 3.557                | -0.233                          | 3.918                            | 3.543                | 0.375                           | -0.347                         |
| A3B8C3              | 3.156                           | 3.449                | -0.293                          | 3.702                            | 3.409                | 0.293                           | -0.335                         |
| A5B10C3             | 5.362                           | 3.201                | 2.161                           | 6.046                            | 3.164                | 2.882                           | -0.412                         |

---

## 6. Discussions

---

The erosion level is closely related to petrographic composition. Carbonate rocks are non-stable rocks and easily eroded. The heterogeneity on petrographic, mineral, chemical composition, texture and structure made difference of expansion coefficient lead to rocks can be more easily destroyed. In the Cat Ba area, there are mainly siliceous-interlaminated limestone and calcilith of Pho Han Formation and dark grey limestone upward to dolomite limestone of Bac Son Formation. Therefore, the petrographic composition of rock controls erosion processes and plays an important role in erosion study.

Rainfall is also an important factor that strongly affected erosion processes on limestones. It can be shown that results of relative erosion rate on some months in the dry season are lower those in the rainy season. It is also equivalent with the trend of total rainfall change measured at Cat Ba Island – according to Cat Ba station rainy months.

In Table 2, initial results show that the relative erosion rate at the stations ranged from 0.196 to 0.282 mm/year. Relative erosion rate value is the lowest at measuring stations X2 on April 8th, 2015 and the highest is at measuring stations Z7 on November 9th, 2015 (Fig. 8), the average value in comparison with previous study results, ranges from  $\pm 0.05$  to  $\pm 0.2$  mm with average eroded level and from  $\pm 0.2$  to  $\pm 0.5$  mm with strong eroded level [8].

In coastal areas and islands, not only erosion process but also accretion process with subtidal and intertidal rock occur. In data processing (Table 6), some negative values are represented as accretion values in the rock surface and some positive values – as erosion values. The research results also

recorded from the accretion process in tropical waves form and form is always submerged stations like Y7, Z1.

Erosion values mainly are recorded at stations in shallow and dry (on land) zone. The intertidal station also has been eroded in some point on surface. Accretion values mainly are recorded in the intertidal zone and subtidal zone.

---

## 7. Conclusion

---

In general, TMEM instrument with high accuracy and precision, low standard deviation [4, 9] plays an important role in erosion studies.

Average relative erosion rates in the study are quite high at some submerged zone stations (about 0.5 mm/year, on average) and quite low with some stations on land in comparison with some previous studies all over the world (Alan S. Trenhaile, 2011) [10]. All results also show the influences of total rainfall on the relative erosion rate of limestone on Cat Ba islands.

The relative erosion rate at the stations ranged from 0.196 to 0.282 mm/year shows that the average value in comparison with previous study results, ranges from  $\pm 0.2$  to  $\pm 0.5$  mm with strong eroded level.

Accretion process also strongly occurs at the intertidal and subtidal (submerged) zone with average annual rate of 0.195 mm/year at station Z1, quite strong accretion level.

---

## Acknowledgement

---

This work was supported by the Vietnam Academy of Science and Technology, Project code VAST05.01/14-15 and BSTMV.06/14-16.

---

## References

1. Minh, N. T. Application of TMEM on study erosion of limestone, Cat Ba island [Text] / N. T. Minh, D. D. Hung, N. H. Hung, L. T. Phuc, N. T. Dung, N. B. Hung et. al. // Proceedings of the 2-nd national scientific conference of Vietnam natural museum system. – Hanoi: Publishing house for science and technology, 2016.
2. Thanh, T. D. Stratigraphic units of Vietnam [Text] / T. D. Thanh, V. Khuc et. al. – Hanoi: Vietnam National Univeristy Publisher, 2005.
3. Phuong, T. H. Initial result in study Devonian-Carboniferous bound at Southern Cat Ba – Hai Phong profile section [Text] / T. H. Phuong, D. N. Truong // Journal of Natural science and Technology. – 2005. – Vol. XXI, Issue 4.
4. Komatsu, T. Devonian-Carboniferous transition containing a Hangenberg Black Shale equivalent in the Pho Han Formation on Cat Ba Island, northeastern Vietnam [Text] / T. Komatsu, S. Kato, K. Hirata, R. Takashima, Y. Ogata, M. Oba et. al. // Palaeogeography, Palaeoclimatology, Palaeoecology. – 2014. – Vol. 404. – P. 30–43. doi: 10.1016/j.palaeo.2014.03.021
5. Inkpen, R. J. Analysis of relationships between micro-topography and short- and long-term erosion rates on shore platforms at Kaikoura Peninsula, South Island, New Zealand [Text] / R. J. Inkpen, W. J. Stephenson, R. M. Kirk, M. A. Hemmingsen, S. A. Hemmingsen // Geomorphology. – 2010. – Vol. 121, Issue 3-4. – P. 266–273. doi: 10.1016/j.geomorph.2010.04.023
6. Inkpen, R. J. The use of multilevel modeling in evaluating controls on erosion rates on inter-tidal shore platforms, Kaikoura Peninsula, South Island, New Zealand [Text] / R. J. Inkpen, L. Twigg, W. J. Stephenson // Geomorphology. – 2004. – Vol. 57, Issue 1-2. – P. 29–39. doi: 10.1016/s0169-555x(03)00081-3
7. Stephenson, W. J. Measuring erosion with the micro-erosion meter – Contributions to understanding landform evolution [Text] / W. J. Stephenson, B. L. Finlayson // Earth-Science Reviews. – 2009. – Vol. 95, Issue 1-2. – P. 53–62. doi: 10.1016/j.earscirev.2009.03.006
8. Moses, C. Methods for measuring rock surface weathering and erosion: A critical review [Text] / C. Moses, D. Robinson, J. Barlow // Earth-Science Reviews. – 2014. – Vol. 135. – P. 141–161. doi: 10.1016/j.earscirev.2014.04.006
9. Spate, A. P. The micro-erosion meter: Use and limitations [Text] / A. P. Spate, J. N. Jennings, D. I. Smith, M. A. Greenaway // Earth Surface Processes and Landforms. – 1985. – Vol. 10, Issue 5. – P. 427–440. doi: 10.1002/esp.3290100504
10. Trenhaile, A. S. Transverse micro-erosion meter measurements; determining minimum sample size [Text] / A. S. Trenhaile, V. C. Lakhan // Geomorphology. – 2011. – Vol. 134, Issue 3-4. – P. 431–439. doi: 10.1016/j.geomorph.2011.07.018
11. Hemmingsen, S. A. The influence of seasonal and local weather conditions on rock surface changes on the shore platform at Kaikoura Peninsula, South Island, New Zealand [Text] / S. A. Hemmingsen, H. S. Eikaas, M. A. Hemmingsen // Geomorphology. – 2007. – Vol. 87, Issue 4. – P. 239–249. doi: 10.1016/j.geomorph.2006.09.010
12. Gomez-Pujol, L. Unravelling factors that control shore platforms and cliffs in microtidal coasts: the case of Mallorcan, Catalanian and Swedish coasts [Text] / L. Gomez-Pujol, E. M. Cruslock, J. J. Fornos, J. O. H. Swantesson // Geomorphologie, Supplementbände. – 2006. – Vol. 144. – P. 117–135.